

Magnetic metamaterials in the blue range using aluminum nanostructures

Yogesh Jeyaram,¹ Shankar K. Jha,¹ Mario Agio,² Jörg F. Löffler,¹ Yasin Ekinci,^{1,3,*}

¹Laboratory of Metal Physics and Technology, Department of Materials, ETH Zurich, 8093 Zurich, Switzerland

²Nano Optics Group, Laboratory of Physical Chemistry, ETH Zurich, 8093 Zurich, Switzerland

³Paul Scherrer Institute, 5232 Villigen-PSI, Switzerland

*Corresponding author: yasin.ekinci@mat.ethz.ch

We report an experimental and theoretical study of the optical properties of two-dimensional arrays of aluminum nanoparticle in-tandem pairs. Plasmon resonances and effective optical constants of these structures are investigated and strong magnetic response as well as negative permeability are observed down to 400 nm wavelength. Theoretical calculations based on the finite-difference time-domain method are performed for various particle dimensions and lattice parameters, and are found to be in good agreement with the experimental results. The results show that metamaterials operating across the whole visible wavelength range are feasible.

In the last decade, a new class of optical materials known as metamaterials have emerged and attracted significant interest. These are metallic structures engineered at the subwavelength scale to exhibit novel optical properties such as negative refractive index or magnetic activity at high frequencies [1]. After the first experimental demonstration in the microwave regime, the operation frequency of metamaterials has experienced a tremendous progress within a decade due to novel designs and nanofabrication techniques [2]. In particular, metal/dielectric/metal multilayers, such as cut-wire nanopairs, fishnet nanostructures, and nanoparticle pairs, have enabled metamaterials operating at optical frequencies. These structures exhibit strong antisymmetric eigenmodes providing magnetic resonances and negative permeability, which is the prerequisite of negative refractive index metamaterials [3, 4, 5, 6, 7]. With such designs magnetic metamaterials at about 1.2 μm have been realized using interference lithography [8]. Record wavelengths of metamaterials have been achieved by Chettiar *et al.* demonstrating negative refractive index at 813 nm and negative permeability at 772 nm [9] and by Yuan *et al.* demonstrating negative permeability at 725 nm [10]. Moreover, 1D-metamaterials have been demonstrated exhibiting a magnetic resonance [11] and a negative permeability [12] at about 630 nm.

In these aforementioned and many other works demonstrating metamaterials with negative refractive index or negative permeability mostly Au and Ag were used, which are, in fact, the conventional choice in plasmonics. On the other hand, Al is also a good optical material because of its low absorption and large real part of the dielectric constant. Whereas Au and Ag exhibit interband absorptions below the wavelengths of about 590 nm and 350 nm, respectively, which limit their applications in optics and plasmonics, Al has low absorption down to 200 nm due to its free-electron-like character and high bulk plasmon frequency [13]. These properties make Al an ideal candidate for plasmonic applications at short wavelengths [14, 15, 16, 17].

In this letter we study the plasmonic properties of ar-

rays of Al in-tandem particle pairs. Ordered 2D arrays of Al/Al₂O₃/Al nanoparticles show strong plasmonic resonances of hybridized eigenmodes due to the near-field coupling between nanoparticles. We demonstrate that it is possible to tune the magnetic resonances down to 400 nm and obtain even negative permeability covering the whole visible range.

Two-dimensional arrays of Al nanoparticles pairs on quartz substrates (HPFS) were fabricated using extreme-ultraviolet interference lithography (EUV-IL) and sequential deposition of Al, Al₂O₃, and Al with a subsequent lift-off process. EUV-IL provides high-resolution structures over large areas with perfect periodicity [18]. Moreover, there is no need for a conduction layer such as ITO which is used in e-beam lithography. Figure 1(a) shows a top-down scanning electron microscope (SEM) image of a typical sample. Figure 1(b) is another SEM image taken at an oblique angle, demonstrating the sandwich-like geometry of the fabricated in-tandem nanoparticle pairs, the schematic cross-section of which is shown in Fig. 1(c). The size of the fabricated structures varied from $2r = 72$ nm to 135 nm (in base diameter) with a fixed period of $a = 200$ nm. The thicknesses of the Al and Al₂O₃ layers were 21 nm and 24 nm, respectively. The area of an array was $400 \mu\text{m} \times 400 \mu\text{m}$, simplifying optical characterization substantially.

Transmission spectra of the structures were measured with a home-made micro-spectroscopy setup, which enables spectroscopy in the visible and UV ranges. The reflection spectra were measured with the same home-made setup in the UV range and with a standard optical microscope in the visible range. Since the structures are isotropic on the substrate plane, no special polarization optics was used. Figures 2(a) and (b) show the transmission and reflection spectra of the samples with different diameters. The transmission spectra exhibit two dips associated with hybridized modes resulting from the dipolar coupling between the individual nanoparticles of a pair. The resonance at shorter wavelengths can be identified as a symmetric resonance or electric dipolar resonance while the one at longer wavelengths is attributed to

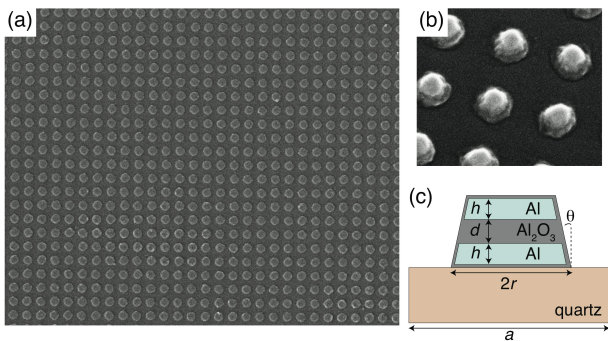


FIG. 1: (a) SEM image of one of the fabricated samples (diameter, $2r = 120$ nm and period $a = 200$ nm). (b) SEM image at an oblique angle with details on the vertical profile of one sample ($h = 21$ nm, $d = 24$ nm, $a = 200$ nm, $\theta = 20^\circ$, $n_{\text{Al}_2\text{O}_3} = 1.77$, $n_{\text{quartz}} = 1.46$, n_{Al} is from [13] and $2r = 135, 120, 105, 87, 82, 72$ nm; a 3-nm-thick Al_2O_3 coating layer is also taken into account).

the antisymmetric or magnetic dipolar resonance [4, 7]. These two resonances are also evident in the reflection spectra (see Fig. 2(b)) where the resonance peaks appear asymmetric due the Fano-type of interference between the eigenmodes [7]. The antisymmetric mode arises due to the induced dipole vectors in the two metal layers being opposite to each other. This creates a magnetic dipole moment which couples to the magnetic component of the incident field and thus gives rise to effective permeability diverging from unity. As seen in Fig. 2(b) the magnetic resonance can be easily tuned by varying the particle diameter for constant metal and dielectric thickness.

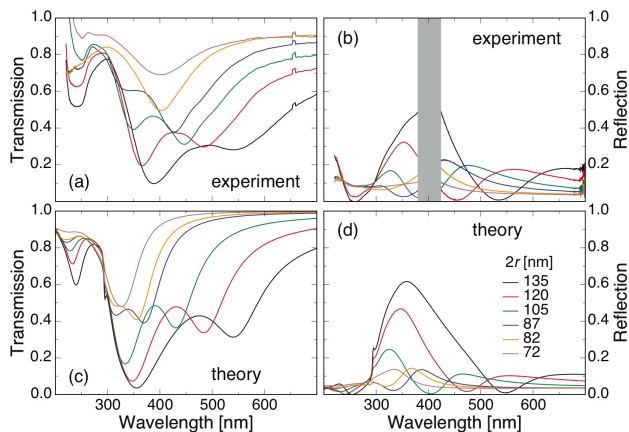


FIG. 2: Transmission ((a) and (b)) and reflection ((c) and (d)) spectra for samples with different disk diameters $2r$. (a) and (c) experimental, (b) and (d) theoretical FDTD results. Note that the reflection spectra in (b) were measured with two different setups (200-400 nm and 400-700 nm). A small range of the spectra (shaded region between 380-420 nm) is not shown because the results were not reproducible because of the low signal-to-noise ratios of both setups in this region.

Finite-difference time-domain (FDTD) simulations were performed using the schematic model shown in Fig. 1(c), which represents relatively simple but realistic structural parameters of the fabricated structures. A natural Al_2O_3 layer of 3 nm is assumed to cover the nanoparticles at the Al-air and Al-substrate interfaces, which is known to be formed immediately when Al is exposed to air or oxygen-rich substrate [19]. For dielectric constants of Al and Al_2O_3 we used the reported values from the literature [13]. Periodic boundary conditions were applied to account for the effects of array on optical response. Figure 2 shows good agreement between the experimental and the calculated spectra, especially for the samples with larger nanoparticles. The small variation between the theoretical and experimental results are due to discrepancies between the exact geometry and optical constants between the modeled and fabricated structures. Moreover, the size and the shape dispersion of the samples resulting from the finite grain size of deposited Al could not be taken into account in the theory.

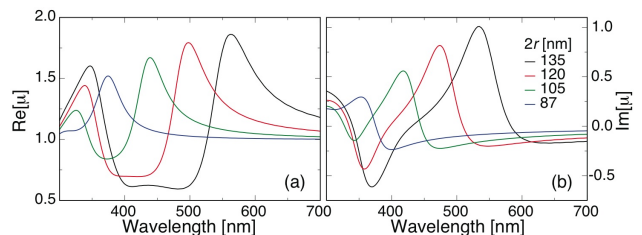


FIG. 3: (a) Real and (b) imaginary part of the relative magnetic permeability μ extracted from FDTD simulations for the fabricated samples.

Since the present structures exhibit significant magnetic resonances we can expect a strong modulation of the effective magnetic permeability. We extracted the effective optical constants from the complex reflectance and transmittance coefficients [20, 21]. Figure 3 displays the complex relative magnetic permeability μ for selected samples. Different nanodisk radii r provide strong magnetic resonances covering the visible and the UV spectral ranges with strong modulations of $\text{Re}[\mu]$ between 0.5 and 2 and without a significant change in the figure of merit $|\text{Re}[\mu]/\text{Im}[\mu]|$. The results show how the amplitude and the wavelength of the effective permeability of the present metamaterial structures can be easily tuned.

Having demonstrated the tunability of the magnetic resonance wavelength, we performed extensive FDTD simulations to optimize the structural parameters in order to study the tunability of the amplitude of the magnetic resonance. Particular interest was paid on achieving negative permeability at short wavelengths within the structural parameters feasible with standard lithographic processes. The extracted μ for some representative cases is shown in Fig. 4. A strong magnetic response is obtained at around 500 nm, with μ as large as 7. A nega-

tive permeability at about 450 nm is achieved, notwithstanding its relatively low figure of merit. As seen in the figure, in changing the lattice parameter from 160 nm to 140 nm, the magnetic resonance of the same nanoparticle pair exhibits a red shift. Similar to electric dipole interactions in nanoparticles arrays [22], we show the evidence of magnetic dipole coupling, which deserves a detailed investigation in future studies.

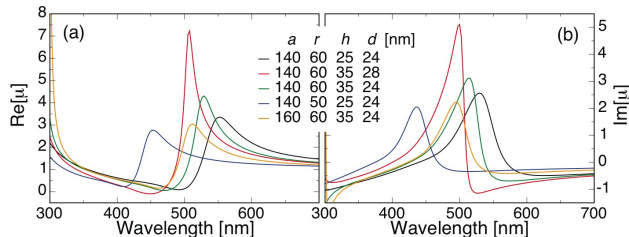


FIG. 4: (a) Real and (b) imaginary part of the relative magnetic permeability μ extracted from FDTD simulations for the structural parameters provided in the legend. The oxide coating has been neglected.

In summary, we have demonstrated that magnetic metamaterials can be obtained down to the blue wavelength range with 2D arrays of Al in-tandem nanoparticles. Thanks to the optical properties of Al, negative permeability is shown to be feasible paving the way towards negative refractive-index metamaterials in the whole visible range. Even though the figure of merit is relatively low, the promise of the present work should invoke further studies with new designs like nanohole array or fishnet structures [23], which may provide negative permeability with a higher figure of merit and even negative refractive index. The Al metamaterials studied in this work also offer new opportunities in other applications of metamaterials, such as in impedance matching to maximize power transfer from vacuum into material [24], magnetic waveguides as building blocks of optical circuitry [25], novel optical materials supporting multiple resonances [5], and as unidirectional optical nanoantennas for surface-enhanced spectroscopy [26].

This work was supported by ETH Research Grant TH-29/07-3. MA thanks Vahid Sandoghdar for continuous support and encouragement. Part of this work was performed at the Swiss Light Source (SLS), Paul Scherrer Institute, Switzerland.

[1] V. M. Shalaev, Nat. Photon. **1**, 41 (2007).

- [2] S. Linden, M. Wegener, and C. M. Soukoulis, Science **315**, 47 (2007).
- [3] Z. Huang, J. Xue, Y. Hou, J. Chu, and D. H. Zhang, Phys. Rev. B **74**, 193105 (2006).
- [4] T. Pakizeh, M. S. Abrishamian, N. Granpayeh, A. Dmitriev, and M. Käll, Opt. Express **14**, 8240 (2006).
- [5] W. Cai, U. K. Chettiar, H.-K. Yuan, V. C. de Silva, A. V. Kildishev, V. P. Drachev, and V. M. Shalaev, Opt. Express **15**, 3333 (2007).
- [6] T. Pakizeh, A. Dmitriev, M. S. Abrishamian, N. Granpayeh, and M. Käll, J. Opt. Soc. Am. B **25**, 659 (2008).
- [7] Y. Ekinici, A. Christ, M. Agio, O. J. F. Martin, H. H. Solak, and J. F. Löffler, Opt. Express **16**, 13287 (2008).
- [8] N. Feth, C. Enkrich, M. Wegener, and S. Linden, Opt. Express **15**, 501 (2007).
- [9] U. K. Chettiar, A. V. Kildishev, H.-K. Yuan, W. Cai, S. Xiao, V. P. Drachev, and V. M. Shalaev, Optics Lett. **32**, 1671 (2007).
- [10] H.-K. Yuan, U. K. Chettiar, W. Cai, A. V. Kildishev, A. Boltasseva, V. P. Drachev, and V. M. Shalaev, Opt. Express **15**, 1076 (2007).
- [11] S. Xiao, U. K. Chettiar, A. V. Kildishev, V. Drachev, I. C. Khoo, and V. M. Shalaev, Appl. Phys. Lett. **95**, 033115 (2009).
- [12] H. Schweizer, L. Fu, H. Gräbeldinger, H. Guo, N. Liu, S. Kaiser, and H. Giessen, Phys. Stat. Sol. (a) **204**, 3886 (2007).
- [13] E. D. Palik and G. Ghosh, eds., *Handbook of Optical Constants of Solids* (Academic Press, 1998).
- [14] Y. Ekinici, H. H. Solak, and C. David, Optics Lett. **32**, 172 (2007).
- [15] K. Ray, M. H. Chowdhury, and J. R. Lakowicz, Anal. Chem. **79**, 6480 (2007).
- [16] Y. Ekinici, H. H. Solak, and J. F. Löffler, J. Appl. Phys. **14**, 083107 (2008).
- [17] A. Mohammadi, V. Sandoghdar, and M. Agio, J. Comput. Theor. Nanosci. **6**, 2024 (2009).
- [18] H. H. Solak, Y. Ekinici, P. Käser, and S. Park, J. Vac. Sci. Technol. B **25**, 91 (2007).
- [19] V. Y. Gertsman and Q. S. M. Kwok, Microsc. Microanal. **11**, 410 (2005).
- [20] D. R. Smith, S. Schultz, P. Markoš, and C. M. Soukoulis, Phys. Rev. B **65**, 195104 (2002).
- [21] V. M. Shalaev, W. Cai, U. K. Chettiar, H.-K. Yuan, A. K. Sarychev, V. P. Drachev, and A. V. Kildishev, Opt. Lett. **30**, 3356 (2005).
- [22] B. Lamprecht, G. Schider, R. T. Lechner, H. Ditlbacher, J. R. Krenn, A. Leitner, and F. R. Aussenegg, Phys. Rev. Lett. **84**, 4721 (2000).
- [23] G. Dolling, M. Wegener, C. M. Soukoulis, and S. Linden, Opt. Express **15**, 11536 (2007).
- [24] J. W. Lee, M. A. Seo, J. Y. Sohn, Y. H. Ahn, D. S. Kim, S. C. Jeoung, C. Lienau, and Q.-H. Park, Opt. Express **13**, 10681 (2005).
- [25] H. Liu, Y. M. Liu, T. Li, S. M. Wang, S. N. Zhu, and X. Zhang, Phys. Stat. Sol. (b) **246**, 1397 (2009).
- [26] T. Pakizeh and M. Käll, Nano Lett. **9**, 2343 (2009).